Journal of Process Control 22 (2012) 809–822

Contents lists available at SciVerse ScienceDirect

Journal of Process Control

journal homepage: www.elsevier.com/locate/jprocont

Stabilization of slugging in oil production facilities with or without upstream pressure sensors

Florent Di Meglio[a,*], Nicolas Petit[a], Vidar Alstad[b], Glenn-Ole Kaasa[b]

[a] Centre Automatique et systèmes, MINES ParisTech, 60 bd St-Michel, 75272 Paris Cedex 06, France
[b] Statoil ASA, Research Center Porsgrunn, Heroya Forskningspark, 3908 Porsgrunn, Norway

ARTICLE INFO

Article history:
Received 27 April 2011
Received in revised form 29 February 2012
Accepted 29 February 2012
Available online 23 March 2012

Keywords:
Slugging
Stabilization
Observer
Multiphase flow

ABSTRACT

This paper presents methods for suppressing the slugging phenomenon occurring in multiphase flow. The considered systems include industrial oil production facilities such as gas-lifted wells and flowline risers with low-points. Given the difficulty to maintain sensors in deep locations, a particular emphasis is put on observer-based control design. It appears that, without any upstream pressure sensor, such a strategy can stabilize the flow. Besides, given a measurement or estimate of the upstream pressure, we propose a control strategy alternative to the classical techniques. The efficiency of these methods is assessed through experiments on a mid-scaled multiphase flow loop.

1. Introduction

This paper studies methods to suppress slugging on oil wells and flowlines by feedback control of the outlet valve. These methods are built around existing approaches of multiphase flow modelling and previously introduced control algorithms. They are relatively general and consistent with automatic control technologies (actuators and sensors) available on industrial facilities. The purpose of this article is to give an overview of the challenges raised by these complex systems, and to outline what can be expected on full-scale systems, in light of mid-scale experiments.

Slugging is an intermittent multiphase flow regime occurring, most frequently, on mature oil fields. It arises from an inhomogeneous distribution of the gas and liquid phases inside transport pipes, and can cause substantial decreases in oil production, resulting in profit losses. Here, we investigate and compare strategies to suppress this phenomenon using pressure sensors in feedback loops.

From an industrial point of view, the main objective of these control laws is to increase the production of oil. One criterion used to compare the performance of each controller is the maximum opening of the production valve around which the system can be stabilized.[1] A larger valve opening corresponds, at steady-state, to a lower pressure inside the pipe. On real oil fields, this will translate into a higher oil production since the reservoir pressure is approximately constant.[2] Another important criterion is the robustness to changes in operating conditions. Both will be the subject of investigations.

Suppression of slugging in the petroleum production industry has been investigated as early as the 1930s (see [1–5]). Active control of the outlet valve has been identified as the most cost-effective solution. If used with a well-chosen information signal, it allows one to counteract the pressure and flow rate oscillations concomitant with the occurrence of slugging, and thus to stabilize the flow. Classically, pressure measurements are used in feedback loops to actuate the valve. The current state-of-the-art strategy is a single-variable (PI) controller using only an upstream pressure sensor (that is to say, a sensor located at the bottom of the pipe), when it is available. Several contributions report successful implementations of such a control method [3,6,7].

However, such a simple controller is not always well suited to deal with the complex dynamics involved in slugging. Since it cannot incorporate anticipation terms,[3] it may have difficulties

[1] However, it is not always possible to see the effect of stabilization on production on experimental setups because, for practical reasons, the flow rate average is usually artificially kept constant.
[2] Actually, the reservoir pressure slowly decreases, with a time constant which is much larger than the phenomena studied here.
[3] E.g. derivative terms are usually discarded due to the noise level on the sensor.

* Corresponding author.
E-mail address: florent.di_meglio@mines-paristech.fr (F. Di Meglio).

0959-1524/$ – see front matter © 2012 Elsevier Ltd. All rights reserved.
doi:10.1016/j.jprocont.2012.02.014

handling oscillations over wide ranges of operating points. Besides, the sensor it relies on may be placed at a location where maintenance is difficult or impossible. Using a model-based approach, we investigate methods to overcome both these difficulties.

In an attempt to gain insight into the causes of the observed instabilities, modeling of the slugging phenomenon has become a focusing point, either in view of testing the efficiency of the aforementioned controllers, or to improve their performance. Simulation-oriented models [8,9], based on Partial Differential Equations (PDE), are able to reproduce accurately the behavior of certain slugging systems. On the other hand, simplified models, based on Ordinary Differential Equations (ODE) [10–12] are sufficient to catch the main features of the behavior and are easier to analyze mathematically. In particular, they reveal a handy tool to derive control laws and build observers. This is the approach we follow in this article, as we develop controllers based on reduced-order models (or the analysis thereof) and test them on mid-scale experimental facilities.

We now describe the main lines of our approach.

To investigate novel control solutions, we rely on a reduced-order model for slugging, introduced in [13]. It consists of a 3-state system of nonlinear ODEs, representing the mass conservation laws in two volumes of gas and one of liquid, and is able to reproduce the pressure and flow rate oscillations corresponding to the slugging behavior.

Then, certain parameters need to be adjusted in order for the model to match accurately the characteristics of a desired system. Thus, a tuning procedure ensures that the steady-state and bifurcation properties of the model fit that of any slugging well or flowline. In view of estimating missing measurements, e.g. when no bottom pressure sensor is available, an observer, using only a topside pressure measurement, is proposed (similarly, e.g. to [14,15]). The structure of the proposed observer resembles a high-gain one [16], but its mechanisms are different. Comparisons with real well data show the relevance of this design. The model is then used to propose an alternative control approach to the state-of-the-art method. More precisely, we propose to change the control variable from what is commonly used in the industry. As will appear, the model dynamics can be decomposed, through a feedback, as an asymptotically stable subsystem with decaying input. In particular, in this analysis, the important role of a specific variable, namely the mass of liquid in the riser is stressed, suggesting that it is a natural choice for the variable to be controlled. Interestingly, the mass of liquid is closely related to the pressure drop between the bottom and the top of the pipe, which can easily be computed when the two considered sensors are available. The stability of the system is investigated using a Lyapunov function, which is a classical tool of nonlinear systems theory [17]. This analysis leads us to consider four possible control strategies (including the reference PI controller on the bottom pressure) which we compare through stabilization experiments on a mid-scale experimental multiphase flow loop.

The article is organized as follows. In Section 2 we describe the slugging phenomenon, both from a physical and dynamical systems viewpoint. In Section 3 we present the simplified model used throughout the paper. In Section 4 we detail the calibration procedure and the observer design. In Section 5 we define four control strategies that result from the design of a presented nonlinear control law. These methods are tested and compared on reported experiments in Section 6. Conclusions are given in Section 7.

2. Slugging in the petroleum production industry

In this section, we describe the slugging phenomenon which can arise during the process of oil production. We start with an overview of the literature by detailing the state-of-the-art in this multiphase flow regime, both from a physical and a dynamical systems standpoints.

2.1. Facilities

During the process of oil production, oil, gas, and water simultaneously flow through transport pipes from the reservoirs to surface facilities. A typical offshore field is depicted in Fig. 1. The multiphase mixture flows from the reservoir through the wells to the sea floor facilities. The length of a well ranges from a few hundred meters to several thousands. Most often, wells have a horizontal section slowly transitioning to a vertical one. At the wellhead, a choke valve, remotely actuated, allows the flow to be controlled. Then, the flowline gathers the production from several wells and transports it, at the seabed, over several kilometers. Eventually, the flowline rises to the surface facilities, where the gas, oil and water phases are separated. Again, an actuated choke valve can be used to control the flow at the top of the riser, before the separation process occurs. The height of the riser ranges from around 100 m to 1 km. The mixture of hydrocarbons and water can be two-phase or three-phase depending on temperature and pressure conditions.

2.2. The slugging phenomenon

2.2.1. Physical description

Slugging, also referred to as slug flow, is an intermittent two-phase (or three-phase) flow regime characterized by an inhomogeneous distribution of the gas and liquid phases. More precisely, elongated bubbles of gas flow through the pipe, separated by "slugs" of liquid. At the outlet, this translates into long periods of very low production of liquid, periodically alternating with high peaks of production, which is problematic for the separation process. Also, the overall production is decreased compared to steady flow regimes, such as the bubbly or annular flows, where oil and gas are produced at constant rates.[4] Moreover, the compressibility of the gas bubbles, and the variation of the weight of the liquid column cause periodical oscillations of the pressure, everywhere in the pipe. These oscillations, which can damage the installation, are actually closely related to the decrease of oil production. For a more detailed description of the phenomenon, the reader is referred to [18], or [19].

Slugging can occur on two subsystems of the setup presented in Section 2.1: wells and risers. Fig. 2 schematically depicts the family of systems that are considered throughout the article.

Flowline risers. In the case of risers, slugging mostly arises when the flowline has a low-point angle just before the vertical section. The slugging is then referred to as "severe", and is very well understood from a physical point of view [20,21]. In particular, Storkaas [12] has suggested that, on these systems, the liquid phase acts as a valve at the low-point, alternatively blocking and letting through the gas. During the blocking phase, the pressure builds up to a critical point, where a blow-out occurs. After a while, the liquid accumulates again and the cycle repeats. The slugs of liquid can be as long as the riser, and there is usually not more than one slug at a time.

Gas-lifted wells. Some wells are activated by gas-lift. A casing is built around the well, and filled with gas. The gas is then injected through a one-way valve at the bottom of the well, lowering the density of the liquid column there. Gas-lift related instabilities have also received much attention and are relatively well understood [22,15].

[4] Actually, the main reason for production losses is that slugging is typically handled by choking back the production to stabilize the flow, i.e. reducing the opening of the outlet valve.

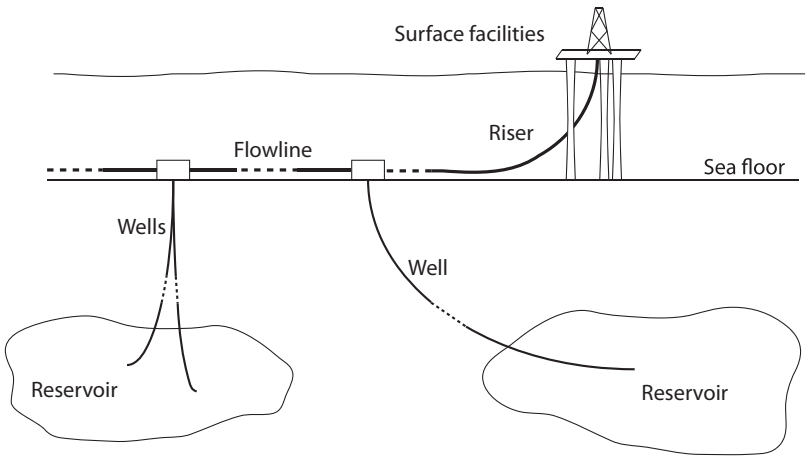

Fig. 1. Schematic view of an offshore field.

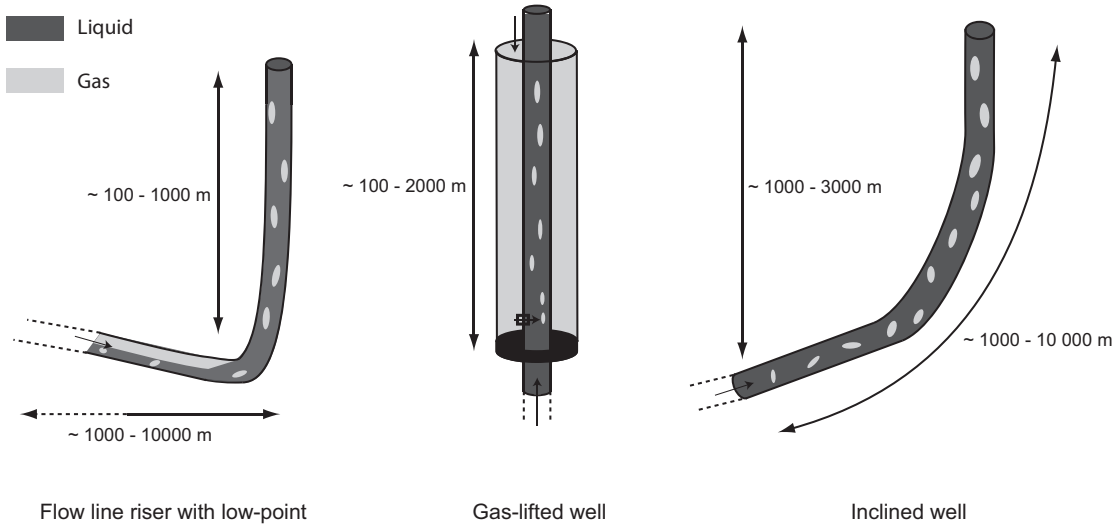

Fig. 2. Types of systems concerned by the slugging phenomenon.

Wells. On some systems, the mechanisms of the slugging phenomenon are poorly understood. In the absence of a low-point or gas-lift, even accurate simulation models may fail to predict the slugging behavior of some wells. In this case, several slugs, smaller than those of the severe slugging, may be present in the riser at the same time.

Although the characteristics of the slugging are different (e.g. the length and speed of the slugs, the hold-up profiles...) for each of these systems, the underlying causes are the same from a dynamical systems point of view, as we will now recall.

2.2.2. Analytical description

From an analytical viewpoint, slugging corresponds to the nonlinear oscillatory behavior of a dynamical system. It can be proved [15], for a simplified model, that a limit cycle exists only when the equilibrium of this system (which is unique) is unstable. In particular, when stabilizing the equilibrium, one suppresses the slugging and the system switches to a steady flow regime. An important feature of slugging systems is that they can be stabilized simply by "choking" the pipe [5], that is to say reducing the opening of the outlet valve, which is the control actuator. Analytically, this corresponds to a Hopf bifurcation [23]. When decreasing the valve opening, the eigenvalues of the system change. At a critical "bifurcation point", they cross the imaginary axis and become stable, and the flow then becomes steady. Unfortunately, choking the pipe increases the pressure in the pipe, and therefore decreases the production since the reservoir pressure is constant.

The effect of this bifurcation on production is pictured in Fig. 3, obtained by simulations on a simplified model, which is a slightly modified version of the one developed in the next section.[5] The production of oil is plotted as a function of the opening of the outlet valve for a theoretical case. Below the bifurcation point (i.e. for choke openings smaller than 15%), the production is constant, equal to its equilibrium value. Above the bifurcation point, the production is intermittent. For a fixed value of the valve opening, it oscillates periodically. The average of these oscillations is compared here to the theoretical steady-state production, which can only be reached by stabilizing the equilibrium.

To investigate control solutions to reach high production operating points, we rely on a model that we detail in the next section.

3. Simplified model for slugging

In this section, we present our model originally proposed in [13]. We recall its origins and discuss the main modeling assumptions.

[5] More precisely, pressure-driven inflows were added to the model of Section 3.

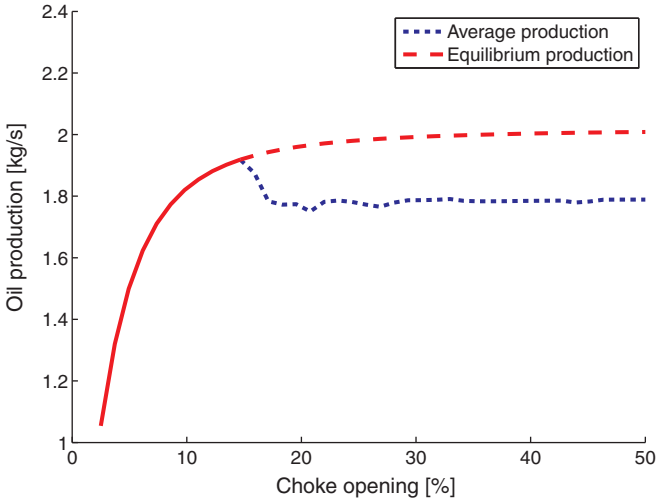

Fig. 3. Average production and equilibrium production versus choke opening. The dashed line corresponds to unstable equilibria. The values of the flow rates and valve opening are only indicative, and do not correspond to any real-world case. This theoretical diagram was obtained by adding a linear relation between the liquid inflow rate and the bottom pressure to the model of Section 3, similarly to [15].

3.1. Origins of the model

The model was largely inspired by those presented in [10,12]. These models are used to reproduce the slugging phenomenon in gas-lifted wells on the one hand and flowline risers with low-points on the other hand. Both have in common that the very nature of the system induces a separation of it into three volumes, not necessarily spatially distinct. In [10], the casing (filled only with gas to be injected in the well) is separated from the tubing (containing one volume of gas, and one of liquid) by the gas injection valve. In the case of the Storkaas model [12], the separation was suggested by the existence of a low-point angle in the geometry of the pipe. The oil, accumulating at the bottom of the riser, acts at this location as a valve for the gas, the opening of which is determined by the height of liquid. In both cases, the gas, accumulating upstream from the separating valve, causes a build-up of pressure, which is the culprit of the instability.

3.2. Model description

Consider now the pipe depicted in Fig. 4. It is subjected to constant inflows of gas and liquid, and the outflow can be controlled thanks to a choke valve. In order to preserve the structure of the Jansen and Storkaas models, which have proved efficient in reproducing the slugging phenomenon for their specific applications, we propose the following new idea: even when the geometry does not suggest such a separation, an irregularity in the pipe may cause the gas to stop flowing steadily. This irregularity is modeled by a 'virtual valve' [13]. Upstream of this virtual valve, gas accumulates and forms a large elongated bubble, where a build-up of pressure occurs, eventually generating instability. The part of the pipe located downstream from the virtual valve will be referred to as the *riser*. We now detail the other modeling assumptions.

Mass balance equations. The state variables are the mass of gas in the elongated bubble $m_{g,eb}$, the mass of gas in the rest of the riser $m_{g,r}$ and the mass of liquid in the riser $m_{l,r}$. Mass conservation reads

$$\dot{m}_{g,eb}(t) = (1-\epsilon)w_{g,in} - w_g(t) \tag{1}$$

$$\dot{m}_{g,r}(t) = \epsilon w_{g,in} + w_g(t) - w_{g,out}(t) \tag{2}$$

$$\dot{m}_{l,r}(t) = w_{l,in} - w_{l,out}(t) \tag{3}$$

where $w_{g,in}$ and $w_{g,out}$ (resp. $w_{l,in}$ and $w_{l,out}$) are the mass flow rates of gas (resp. liquid) entering (*in*) the riser and coming out (*out*) of the riser; and w_g is the mass flow rate of gas through the virtual downhole choke. Note that, in this model, a fraction of the gas flow (determined by $\epsilon \in (0, 1)$) goes directly into the upper part of the riser (along with the liquid), whereas the remaining accumulates in the bottom part of volume V_{eb}, causing a build-up of pressure.

Description of mass flows. As mentioned above, the inflow rates of gas and liquid are assumed constant. This strong assumption is a source of steady-state errors, since, in practice, the inflow rates depend on the operating point, as explained in Section 2.2.2. However, even a linear model of the inflow, such as the one used in [11], dramatically complicates the tuning procedure presented in

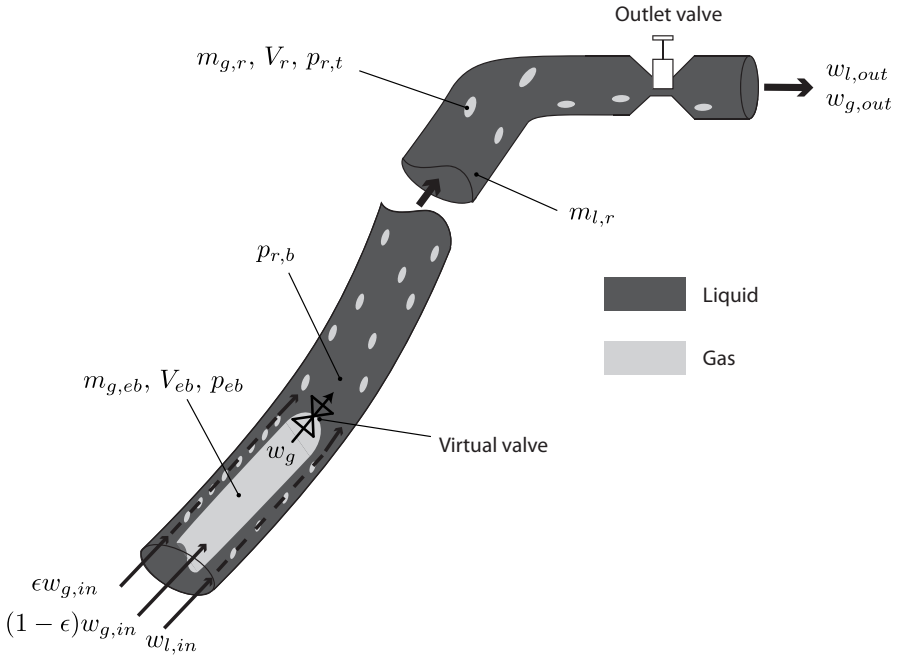

Fig. 4. Schematic view of the considered transport pipe.

Section 4.1. For the gas flow through the virtual valve, we assume a linear relation

$$w_g = C_g \max(0, (p_{eb} - p_{r,b}))$$

where p_{eb} is the pressure in the elongated bubble, and $p_{r,b}$ the pressure in the riser downstream from the valve. C_g is assumed constant, which means that the virtual valve is either fully closed or fully opened. The $\max(0, \cdot)$ function indicates that no back-flow is admitted through the valve. The total flow through the outlet valve is given by a classical valve equation [24]

$$w_{out} = C_{out} u \sqrt{\rho_m (p_{r,t} - p_s)}$$

The density of the mixture ρ_m is assumed constant, equal to the density of the liquid ρ_l. This error will be corrected by tuning parameter C_{out}, as indicated in Section 4.1. On the other hand, p_s is the (constant) separator pressure/manifold pressure, whereas $p_{r,t}$ is the pressure at the top of the riser, upstream from the production valve. u is the opening of the choke, which is the actuator of the system, and C_{out} is the choke constant. The flow rates of gas and liquid are computed from their respective mass fractions

$$w_{l,out} = \frac{m_{l,r}}{m_{l,r} + m_{g,r}} \approx w_{out}$$

$$w_{g,out} = \frac{m_{g,r}}{m_{l,r} + m_{g,r}} \approx \frac{m_{g,r}}{m_{l,r}} w_{out}$$

Closure relations on the pressures. The pressures in the riser are determined by the ideal gas law. To simplify the mathematical analysis, the volume of the elongated bubble V_{eb} is assumed constant. This is consistent with the Jansen and Storkaas models. In the case of gas-lift, the elongated bubble is actually the casing, which has a constant volume. In the case of risers with low-points [12], this assumption is justified by neglecting the liquid dynamics upstream from the low point. Conversely, the gas downstream from the virtual valve is assumed compressible. Its volume is determined by the amount of liquid in this part of the riser: $V_{g,r} = V_r - (m_{l,r}/\rho_l)$, where V_r is the volume of the riser. Friction is neglected, which is a common assumption, as slugging is known to be a gravity-dominated process.

$$\begin{aligned} p_{eb} &= \frac{m_{g,eb} RT}{M V_{eb}} \\ p_{r,t} &= \frac{m_{g,r} RT}{M(V_r - (m_{l,r} + m_{l,still}/\rho_l))} \\ p_{r,b} &= p_{r,t} + (m_{l,r} + m_{l,still}) \frac{g \sin\theta}{A} \end{aligned} \tag{4}$$

θ is the mean inclination of the pipe, and A the cross-section area. One should note that the effect of the mass of gas on the gravity pressure drop is neglected, compared to that of the mass of liquid. $m_{l,still}$ is a constant parameter used for tuning purposes. It represents the minimum mass of liquid present in the riser at all times. Indeed, apart from the case of severe slugging (where $m_{l,still}$ may be 0), the riser is never filled only with gas, and only part of the liquid is concerned by the dynamics (1)–(3). Finally, the temperature is assumed constant throughout the pipe and in time.

As detailed in [13,25], this model features a Hopf bifurcation similar to that of slugging systems. Its unique equilibrium is unstable for large valve openings, and its trajectories converge to a limit cycle which corresponds to the slugging oscillations. In the next Section, we detail how to ensure that the characteristics of this limit cycle match that of an observed slugging system.

4. Parameter tuning and observer design: a case study

To illustrate the relevance of the proposed model, we now present how to ensure that it matches the slugging features of a given system. In Section 4.1, we propose a method to calibrate the parameters of the model, based on its dynamical properties. Then, in Section 4.2, we design an observer allowing the reconstruction of unmeasured states using a topside pressure sensor only, in view of using them for control. The calibration and observer are tested on experimental data corresponding to an actual well in the Oseberg field, in the North Sea.

4.1. Parameter tuning

As mentioned earlier, the characteristics of the slugging vary from one system to the next. The frequency, shape, and magnitude of the oscillations, for example, significantly differ when considering a well or a flowline riser. To ensure that the model matches the slugging features of a given system, certain parameters need to be adjusted. Because the parameters do not appear linearly in the model, traditional identification methods from the linear control theory (see e.g. [26]) do not apply. Rather, we propose an off-line procedure consisting in fitting one-by-one certain characteristics of the bifurcation diagram of the model to that of the considered system. This method has the following advantages.

- By carefully choosing the order with which the parameters are calibrated, this method results in a triangular set of nonlinear equations to be solved. One parameter can be identified at a time, and the procedure is, for the most part, analytical.
- Fitting the characteristics of the bifurcation diagram allows the model to be representative of the considered system for a broad range of operating points. Thus, the non-slugging behavior of the model can also be close to the non-slugging behavior of the real system (steady-state errors are thus limited to a minimum). This would not have been guaranteed by a method consisting, e.g. in identifying the parameters using data from a single slugging operating point.
- Interestingly, the method indicates how to plan the experimental validation. It requires measurements from several operating points and several sensors which must be obtained from preliminary tests.

We now detail the method we use to give values to the 16 parameters of the model.

1. 8 parameters do not require any calibration: θ, A, g, ρ_l, R, T, M and p_s are known or can be accurately measured for all systems.
2. The parameter V_r, which represents the volume of the riser, corresponds to the position of the virtual valve.
3. The inflow rates of gas and liquid are *a priori* unknown. However, they can be set equal to the average productions of gas and liquid during slugging at a given operating point. Notice however that these do not correspond to the levels of production in non-slugging flow,[6] which may cause a small steady-state error.
4. The last 5 parameters are calibrated using the bifurcation diagram. Fig. 5, which summarizes this step, pictures the equilibrium curve of the bottom pressure as a function of the valve opening for the well of the Oseberg field. The analytical formulas used to determine the values of the parameters are given in Appendix A.

Remarks on the tuning process. The only parameter whose effect is not direct from an physical viewpoint is the virtual valve constant C_g. It affects the shape of the oscillations, which can only be seen after the last parameter (V_{eb}) has been chosen. A trial-and-error

[6] The production is higher in non-slugging flow, which is actually the reason for stabilizing the system!

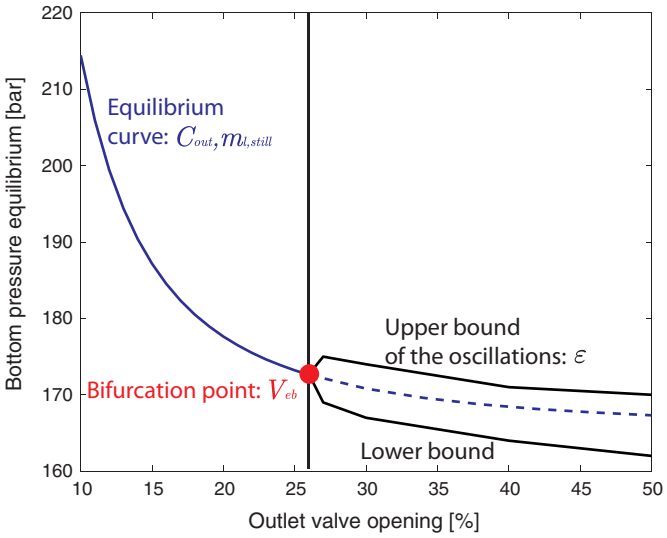

Fig. 5. Bifurcation diagram of the bottom pressure. The values of parameters C_{out} and $m_{l,still}$ are determined using the steady-state values of the topside and bottom pressures, respectively, at one operating point. This ensures that the equilibrium curves of the model and the real system match at the vicinity of this point. The value of parameter V_{eb} directly determines the position of the bifurcation point. Finally, ϵ is related to the amplitude of the oscillations.

method is necessary to find the value for C_g that matches best the observed system, re-computing at each step the value of V_{eb}.

Another important feature of this procedure is that it only requires steady-state information about the bottom pressure. This is crucial when no bottom pressure sensor is available. In that case, the equilibrium pressure can (and must) be estimated by an advanced multiphase-flow model, such as OLGA^{TM}. The rest of the information needed to complete the procedure is available topside, but may involve performing preliminary experiments on the system under study.

For more detailed explanations on the tuning procedure, the interested reader is referred to [27]. Once it has been completed, the model can be used to estimate missing measurements, using the observer proposed in the next section.

4.2. Observer design

The structure of the proposed observer resembles a high-gain one [16]. To highlight this feature, one shall rewrite the model using the measured output as a state variable. Using the following set of state variables $(x_1, x_2, x_3) = (m_{eb}, p_{r,t}, m_{l,r})$, the model is rewritten

$$\begin{aligned}\dot{x}_1 &= f_1(x)\\ &= (1-\epsilon)w_{g,in} - C_g \max\left[0, ax_1 - x_2 - c(x_3 + m_{l,still})\right]\end{aligned} \tag{5}$$

$$\begin{aligned}\dot{x}_2 &= f_2(x)\\ &= \frac{b}{m_l^{\Delta} - x_3}\left[\epsilon w_{g,in} + C_g \max(0, ax_1 - x_2 - c(x_3\right.\\ &\left. + m_{l,still})) + w_{l,in}\frac{x_2}{b} - \frac{m_l^{\Delta}}{x_3}\frac{x_2}{b}uC_{out}\sqrt{\rho_l(x_2 - p_s)}\right]\end{aligned} \tag{6}$$

$$\begin{aligned}\dot{x}_3 &= f_3(x)\\ &= w_{l,in} - C_{out}u\sqrt{\rho_l(x_2 - p_s)}\end{aligned} \tag{7}$$

with

$$a = \frac{RT}{MV_{eb}}, \quad b = \frac{\rho_l RT}{M}, \quad c = \frac{g\sin\theta}{A}, m_l^{\Delta} = \rho_l V_r - m_{l,still} \tag{8}$$

$p_{r,t} = x_2$ is the measured output. The following observer is now considered

$$\dot{\hat{x}}_1 = f_1(\hat{x}) \tag{9}$$

$$\dot{\hat{x}}_2 = f_2(\hat{x}) - k(\hat{x}_2 - x_2) \tag{10}$$

$$\dot{\hat{x}}_3 = f_3(\hat{x}) \tag{11}$$

4.2.1. Remarks on the convergence of the proposed observer

The convergence of this algorithm is rather difficult to study, mainly because of the abrupt periodic changes in the dynamics caused by the openings and closings of the virtual valve. More precisely, the limit cycle of the system has to be separated into two distinct phases, depending on the argument of the $\max(\cdot, 0)$ functions being positive or negative (which corresponds to an open or closed virtual valve). When the observer is not perfectly initialized, it may be in a different zone of the plane-phase from the original system. Thus, there is a total of four combinations to study to establish the convergence of the error dynamics, according to which phase the observer and the original system are in. The mechanisms of the synchronization of the observer and the observed systems are yet to explain. Another difficulty is that across the switch plane (defined by $\{ax_1 - x_2 - c(x_3 + m_{l,still}) = 0\}$), the right-hand side of the dynamics is continuous, but not C^1, which complicates the stability analysis.

Another important feature of this observer is that it does not behave like a high-gain observer. In particular, an analysis of the linearized dynamics around the limit cycle reveals that one of the eigenvalues of the observer goes to 0 as the observer gain, k, goes to infinity. Fortunately, large gains are not necessary as the observer exploits the presence of nonlinear terms which naturally "help" its convergence.

In order to prove the convergence of the full observer scheme, possible directions include the patching of Lyapunov functions [28], the use of regularization functions or the design of a non-smooth Lyapunov function [29]. We now present numerical simulations that validate the relevance of the design.

4.3. Numerical validation of the tuning procedure and observer design

The method was tested on data from a 7731-m-long well located in the North Sea, pictured in Fig. 6. This data demonstrates slugging even though it is recorded at low sample rates and with quantization. The tuning procedure was first applied to the model, using the data pictured in red in Fig. 7. The virtual valve is assumed to be located at the transition between the horizontal part of the riser and the vertically inclined part. Conveniently, this also corresponds to the position of the bottom pressure sensor, which we used *for tuning and comparison only* (i.e. not in the observer). The values of the parameters are listed in Appendix A. Fig. 7 shows the comparison between the actual topside pressure (used in the observer) and the actual bottom pressure on one hand, and the estimates from the model on the other. The low sampling and quantization of the bottom pressure data from the well is only due to database compression.

Should the bottom sensor fail, the estimates can be used to stabilize a slugging system. This point will be highlighted by two of the control solutions presented in the next Section, where several strategies for stabilization of slugging are considered.

5. Control solutions perspectives

In this section, we present the four control strategies (Controllers 1–4) that will be the subject of comparative experiments in Section 6. After recalling the state-of-the-art solution, which

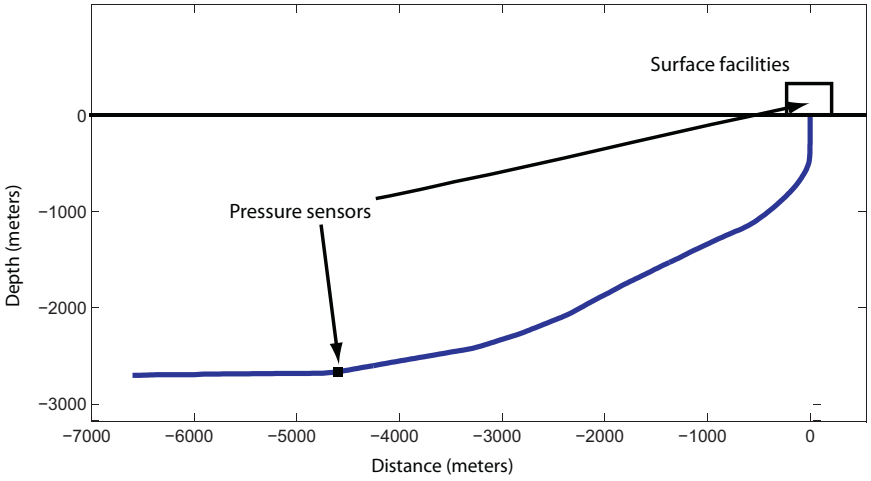

Fig. 6. Schematic view of the geometry of the considered well.

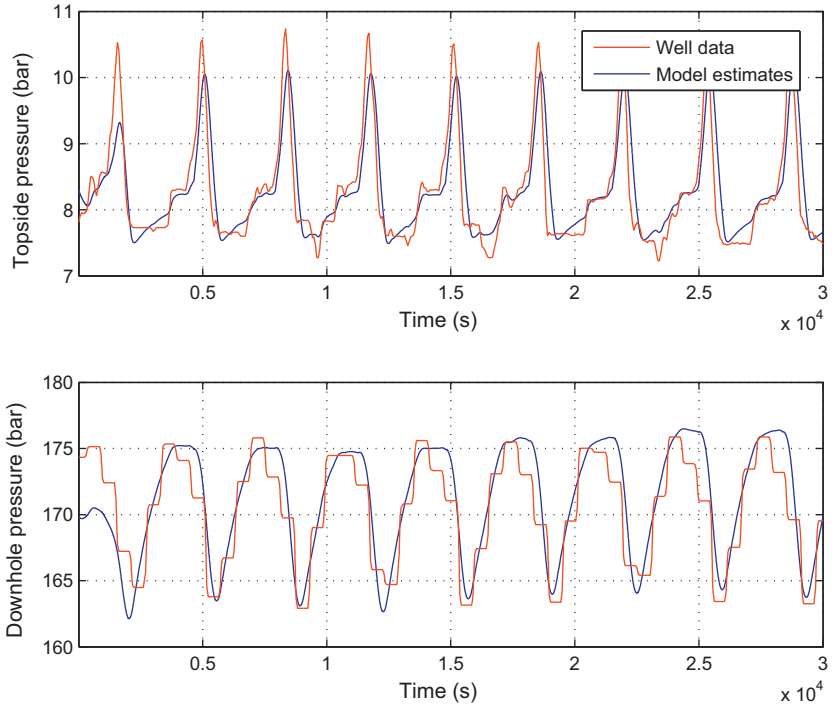

Fig. 7. Comparison between real measurements and observer estimates. The observer gain is $k = 0.1$. (For interpretation of the references to color in the text, the reader is referred to the web version of the article.)

corresponds to Controller 1, we propose an alternative control variable for Controller 2. Then, Controllers 3 and 4 provide solutions relying on the observer presented in Section 4.2, which can be implemented even without a bottom pressure sensor.

5.1. Controller 1: PI controller on the bottom pressure

As mentioned in Section 1, the state-of-the-art control strategy consists of applying a PI feedback control law using the bottom (or riser base) pressure as the output. Several successful implementations of this method are reported in the literature [6,7], and specific tuning rules for the proportional and integral gains of the PI can be found in [3]. The major drawback of this method is that it relies on the availability of a bottom pressure sensor: when the sensor fails, as reported in [6], the slugging starts again. Most importantly, its performance, in terms of production gains could desirably be increased.

5.2. Controller 2: PI controller on the pressure drop over the riser

In [30], the authors achieve stabilization of an experimental slugging riser with low point using the pressure drop over the riser as the output of a PI feedback law. Remarkably, very few other attempts to implement such a controller are reported in the literature. One should notice that it requires a bottom pressure sensor, similarly to Controller 1.

Interestingly, this control variable is closely related to a state variable of our model, the mass of liquid in the riser, which has a particular role in the dynamics of the system. This point will be highlighted by the feedback law derived in Section 5.4.

5.3. Controller 3: PI controller on the estimated pressure drop over the riser

This controller is very similar to Controller 2, only it uses the estimates from the observer (9)–(11) presented in Section 4.2, which are computed using the topside pressure sensor only. This solution allows one to stabilize slugging even in the absence of a bottom pressure sensor.

Besides, the comparison of the performance of Controller 3 versus that of Controller 2 gives a direct estimate of how much (in a sense that will be detailed in Section 6) the model alone can compensate for the unavailability of a bottom pressure sensor.

5.4. Controller 4: a nonlinear stabilizing control law

In this section, we propose a nonlinear control law for the model described in Section 3. The main effect of this feedback law is to linearize the dynamics of the mass of liquid in the riser. Its convergence properties are stated in the following proposition and a sketch of the proof of convergence, detailed in [25], is given below.

Proposition 5.1. *Consider system (5)–(7). The partially linearizing feedback law (Controller 4)*

$$u(t) = \frac{w_{l,in} + k(x_3(t) - \bar{x}_3)}{C_{out}\sqrt{\rho_l(x_2(t) - p_s)}} \tag{12}$$

with $k>0$ stabilizes the system around its equilibrium point $(\bar{x}_1, \bar{x}_2, \bar{x}_3, \bar{u})$ (given in Appendix B) which is Locally Asymptotically Stable.

Elements of Proof The closed loop equations read, from (5)–(7) and (12)

$$\dot{x}_1 = (1-\epsilon)w_{g,in} - C_g \max(0, ax_1 - x_2 - c(x_3 + m_{l,still})) \tag{13}$$

$$\dot{x}_2 = \frac{b}{m_l^{\Delta} - x_3}\left[\epsilon w_{g,in} + C_g \max(0, ax_1 - x_2 - c(x_3 + m_{l,still})) + w_{l,in}\frac{x_2}{b} - \frac{m_l^{\Delta}}{x_3}\frac{x_2}{b}[w_{l,in} + k(x_3 - \bar{x}_3)]\right] \tag{14}$$

$$\dot{x}_3 = -k(x_3 - \bar{x}_3) \tag{15}$$

The local asymptotic stability of the equilibrium of system (13)–(15) can be proved by considering the following candidate Lyapunov function, as done in [25]

$$V = \frac{1}{2}\left(\tilde{x}_1^2 + \tilde{x}_2^2 + \tilde{x}_3^2\right) \tag{16}$$

A conservative estimate of the basin of attraction of the equilibrium can then be constructed by considering the intersection of a level set of V with the region where the right-hand-sides of Eqs. (13)–(15) are smooth functions of the state. The interested reader is referred to [25] for technical details.

Proposition 5.1 stresses the particular role of the x_3 variable, which corresponds to the mass of liquid in the riser. This result is all the more interesting as, even though the mass of liquid cannot be directly measured, it is closely related to the pressure difference between the bottom and the top of the riser. Indeed, let $\Delta P_{riser} = p_{r,b} - p_{r,t}$ be the pressure drop over the riser. According to the model, the following exact affine relation holds

$$\Delta P_{riser} = (m_{l,r} + m_{l,still})\frac{g\sin\theta}{A}$$

In practice, this relation is only approximate since friction and dynamical effects were neglected. However, the pressure drop over the riser can be directly computed from the measurements of the bottom and topside pressure. This suggests that a PI controller on this variable (Controller 2) is an easily implementable potentially efficient solution to stabilize slugging, as will be illustrated in the experiments of Section 6.

Besides, to implement the control law (12), the estimated values of the states $\hat{x}_2$ and $\hat{x}_3$ provided by the observer (9)–(11) are used.

6. Experimental results

In this section, we present experiments performed on mid-scale experimental facilities. We compare the performances of the four control solutions detailed above.

Experimental setup. The experiments are conducted on a 100 m-long, 15 m-high multiphase flow loop located in Porsgrunn, Norway. The pipe is filled at constant rates with air and water, playing the role of gas and oil, respectively.[7] Even under these steady inflow conditions, the loop is able to reproduce the slugging behavior. Fig. 8 shows a schematic view of the geometry of the system, along with a plot of the observed pressure oscillations. For all the reported experiments, the inflow rates are 4 m^3/h for the liquid, and 27 kg/h for the gas.

Criterion for comparison. From an industrial point of view, the main objective of the four studied control laws is to increase the production of oil. However, it is not always possible to see the effect of stabilization on production in experimental setups because, for practical reasons, the flow rate average is usually artificially kept independent of the operating point. Thus, in a such context, the criterion used to compare the performances of each controller is the maximum opening of the production valve around which the system can be stabilized. A larger valve opening corresponds, at steady-state, to a lower pressure inside the pipe, which will translate, in real oil fields, into a higher oil production.

6.1. Experiments

Preliminary experiments. To determine the position of the bifurcation point, and collect data for model tuning, preliminary experiments are needed. Fig. 9 depicts the corresponding data. The opening of the outlet valve is progressively decreased from a slugging operating point until the stable region is reached. Further experiments revealed that 26% was an unstable operating point, which implies that the bifurcation point is approximately 25%. This data was used to determine the parameters of the model according to the procedure described in Section 4.1. The corresponding values are listed in Table A.2. The observer algorithm presented in Section 4.2 was then implemented. Fig. 10 pictures a comparison of the estimates from the model with actual measurements at a fixed valve opening. One should notice the high frequency oscillations appearing in the topside pressure, which are due to hydrodynamic slugging. As mentioned in Section 4.2.1, the observer gain does not need to be large to yield good filtering properties. This is crucial in the implementation of the nonlinear feedback law (Controller 4).

The following experiments correspond, for each controller, to the highest valve opening around which we managed to stabilize. Thus, two aspects of the performances of the controller can be compared in light of these results. First, they give indications of which controller will yield the largest production increases on a real well. Besides, they give an indication on how robust each controller is to changes in operating conditions.

Controller 1: PI on the bottom pressure. Fig. 11 displays the results of the experiment corresponding to the highest unstable valve opening around which Controller 1 was able to stabilize the flow.

[7] Low-level controllers ensure that the inflows are kept constant, to avoid wear and tear on the injection pumps.

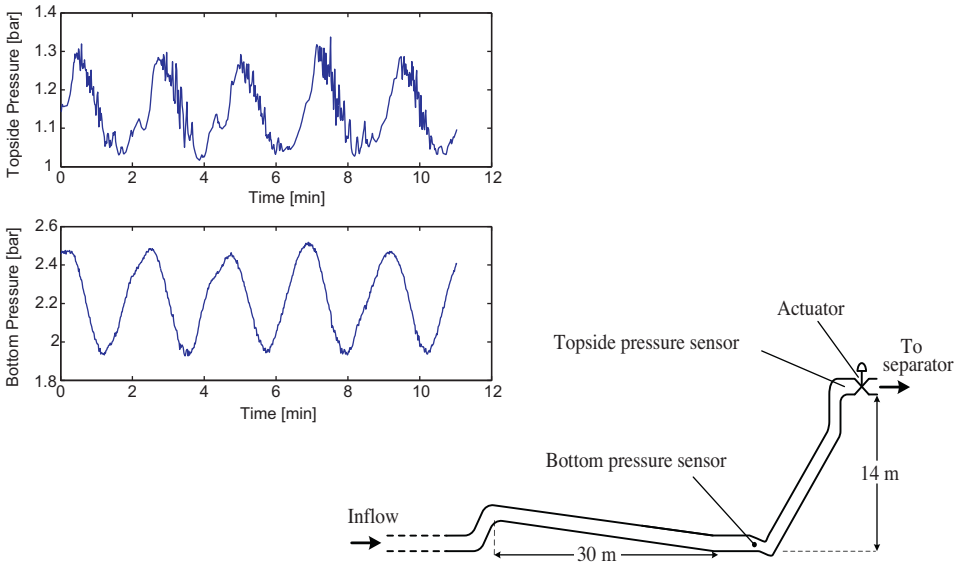

Fig. 8. Schematic view of the riser and open-loop oscillations of the topside and bottom pressures.

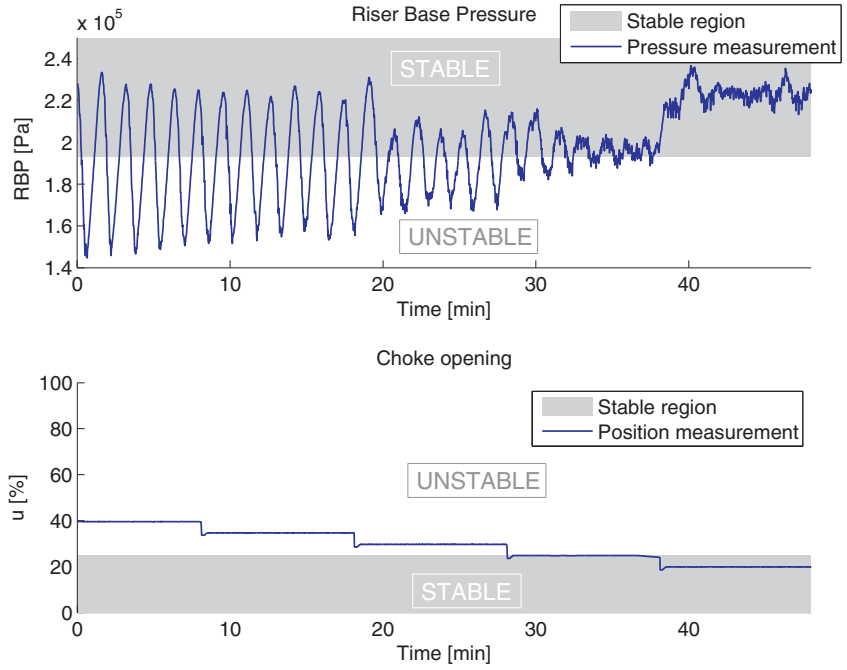

Fig. 9. Preliminary open-loop experiments. The upper plot pictures the measurement from the bottom pressure sensor. The bottom plot pictures the valve position measurement.

Remarkably, the corresponding operating point (26% valve opening) is located very close to the stable region (25% valve opening), which would translate into a relatively minor increase of the production on a real well. Attempts to stabilize at higher operating points have failed, both with the same set of PI controller parameters and different sets. Importantly, Controller 1 reveals sensitivity to the starting time of the controller. It may or may not stabilize the system at 26% valve opening depending on which part of the slugging cycle the system is at when the controller is turned on (which is consistent with the results presented in [31]). This indicates that Controller 1 yields a rather small basin of attraction, and that it is poorly robust to changes in operating conditions.

Controller 2: PI on the pressure drop over the riser. Fig. 12 displays the results of the experiment corresponding to the highest unstable valve opening around which Controller 2 was able to stabilize the flow. The performance of Controller 2 is strikingly better than that of Controller 1, as the flow is stabilized around a 36% valve opening. Remarkably, the same set of PI controller parameters also yields stabilization for smaller valve openings, which shows that this method is relatively robust to changes in operating conditions.

However, stabilization is not perfectly achieved since relatively large pressure oscillations persist. Their magnitude is around.2 bar, which represents a third of the magnitude of the oscillations without control. Besides, their period is approximately 70 s, against 90 s for the slugging oscillations. Most likely, the controller only modifies the limit cycle by significantly reducing the magnitude and altering the frequency of the oscillations. Most importantly, it also

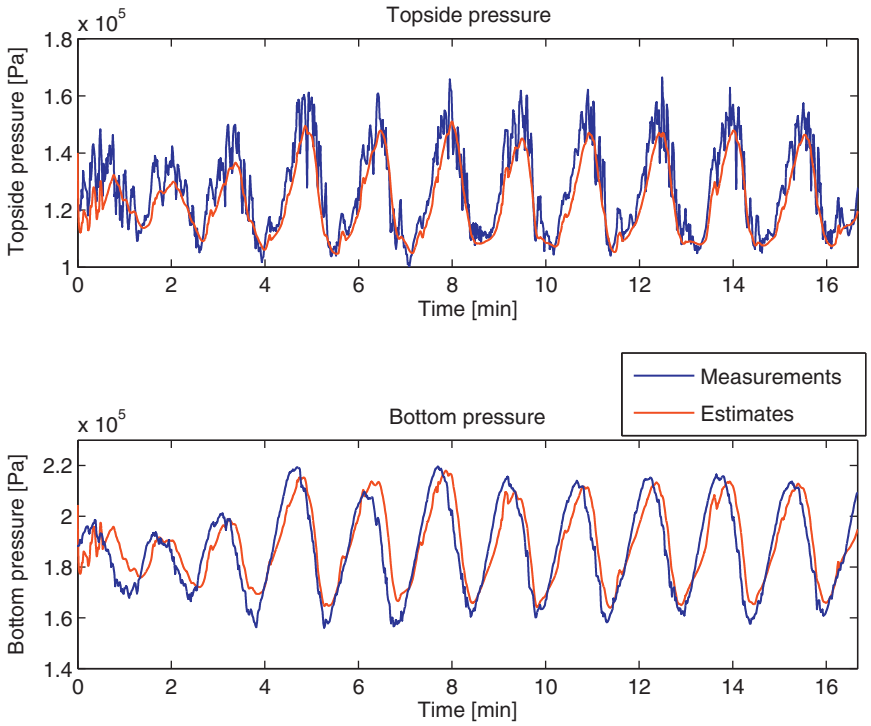

Fig. 10. Comparison between measurements and observer estimates at a 30% valve opening. The topside pressure estimate is $\hat{x}_2(t)$ from the observer (9)–(11) and the bottom pressure estimate is computed from $\hat{x}$ using (4).

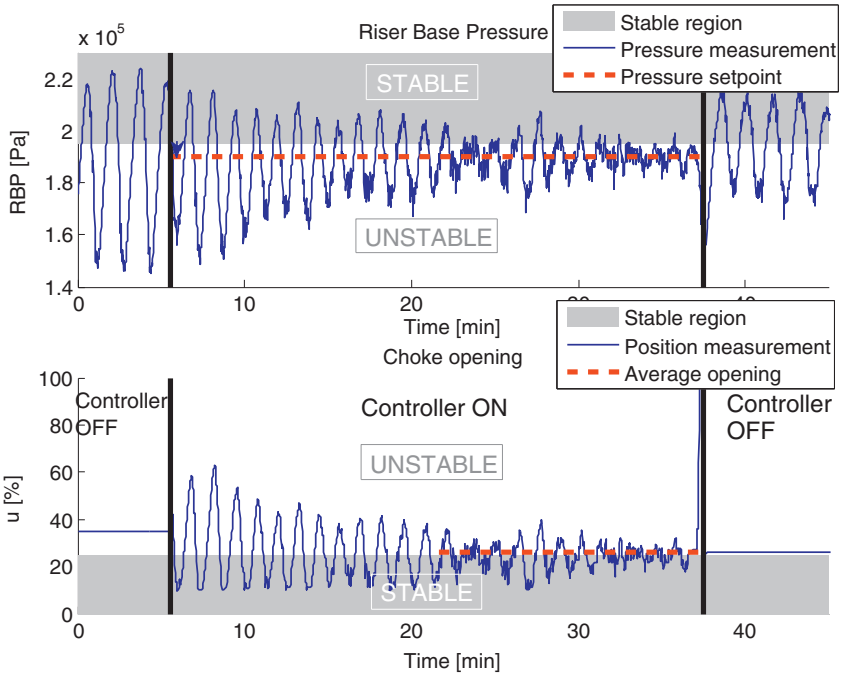

Fig. 11. Stabilization result for the PI on bottom pressure. The average valve opening after stabilization is 26%, right above the bifurcation point.

centers the oscillations around the equilibrium pressure, which should yield production increases on a real well.

For comparison purposes, Fig. 13 pictures the stabilization with the same controller around a 30% choke opening, which yields much smaller residual oscillations.

Controller 3: PI on the estimated pressure drop over the riser. Fig. 14 pictures the experiment corresponding to the maximum valve opening around which Controller 3 could stabilize. As could be expected, the observer does not compensate fully for the absence of a bottom sensor. The highest stabilized operating point is 30%, which is lower than with Controller 2 (36%). This indicates that Controller 3 yields a smaller basin of attraction than Controller 2, and is less robust to changes in operating conditions. However, it is still higher than Controller 1, which confirms the efficiency of controlling the pressure drop over the riser rather than the bottom pressure.

Controller 4: partially linearizing feedback law. Fig. 15 pictures the stabilization experiment corresponding to the highest valve

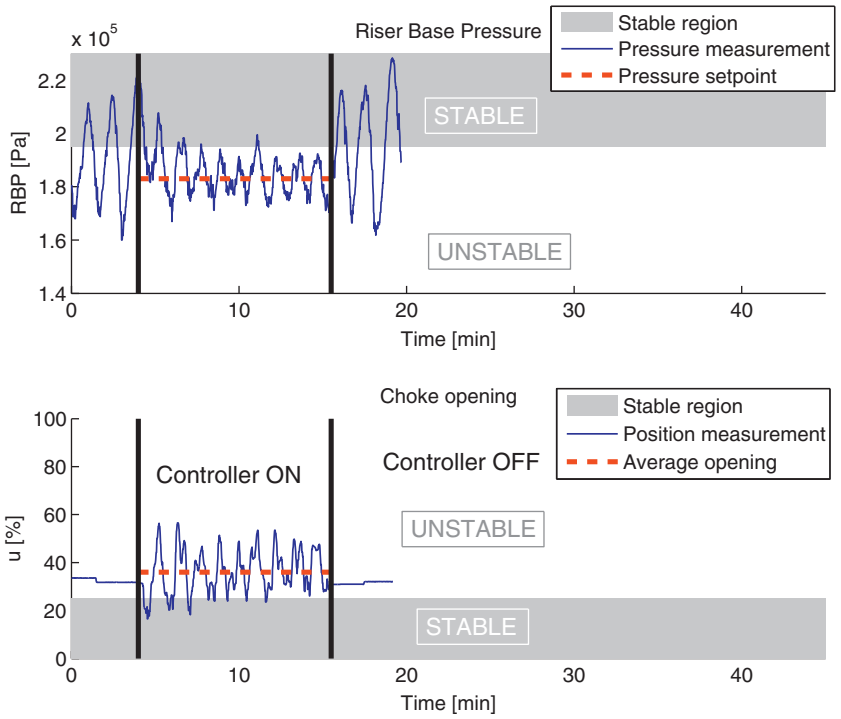

Fig. 12. Stabilization result for the PI on the pressure drop over the riser. The average valve opening after stabilization is 36%.

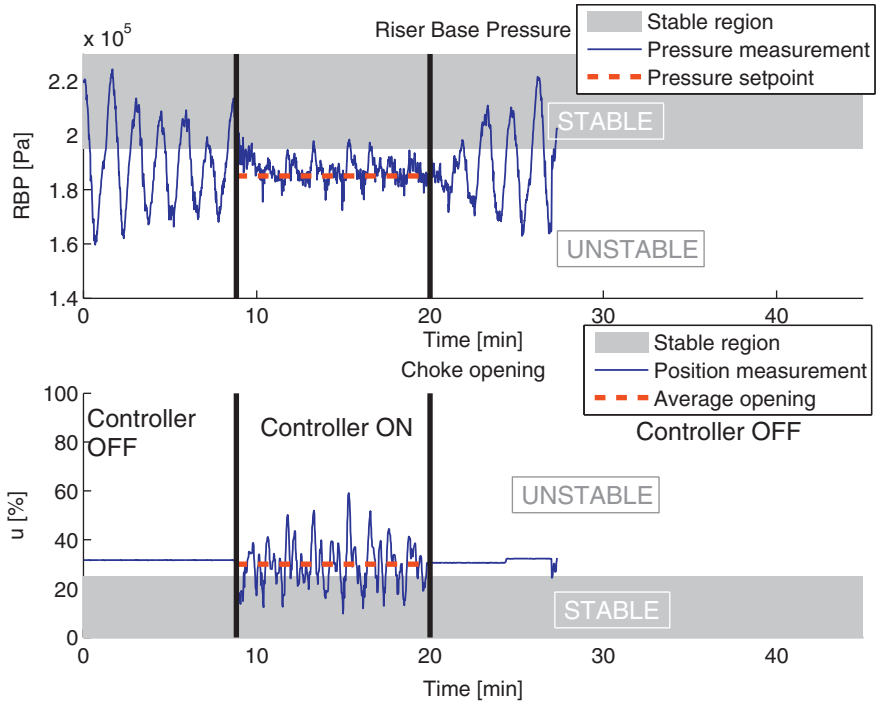

Fig. 13. Stabilization with the PI controller on the pressure drop over the riser around 30%.

Table 1
Summary of the results of the experiments.

#	Pressure sensor(s) used	Control variable	Maximum valve opening
1	Bottom	Bottom pressure	27%
2	Bottom &topside	Pressure drop over the riser	36%
3	Topside	Estimated pressure drop over the riser	30%
4	Topside	Estimated states of the model	35%

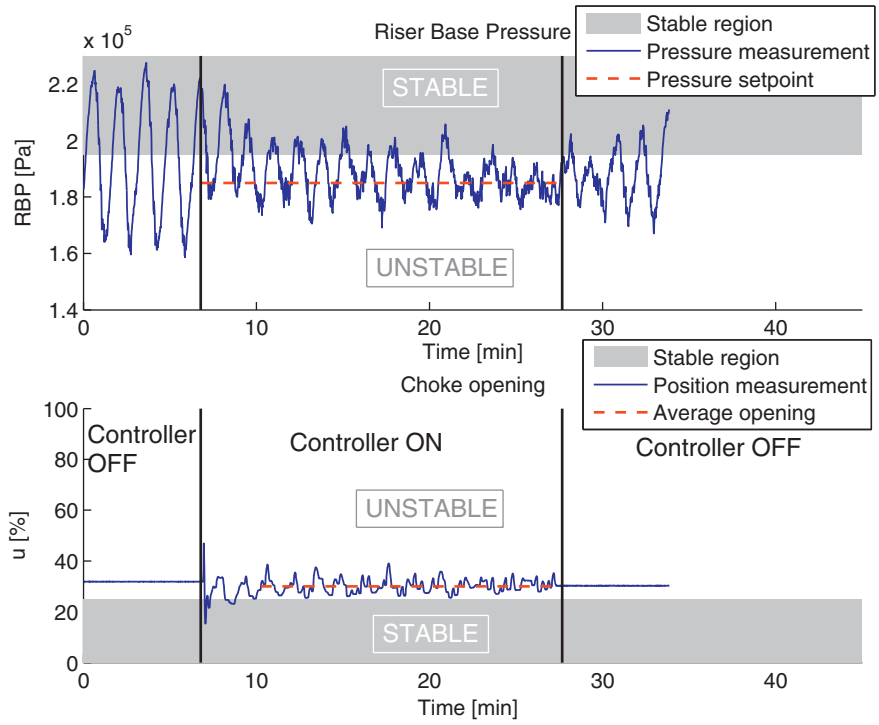

Fig. 14. Stabilization result for the PI on the estimated pressure drop over the riser. The average valve opening after stabilization is 30%.

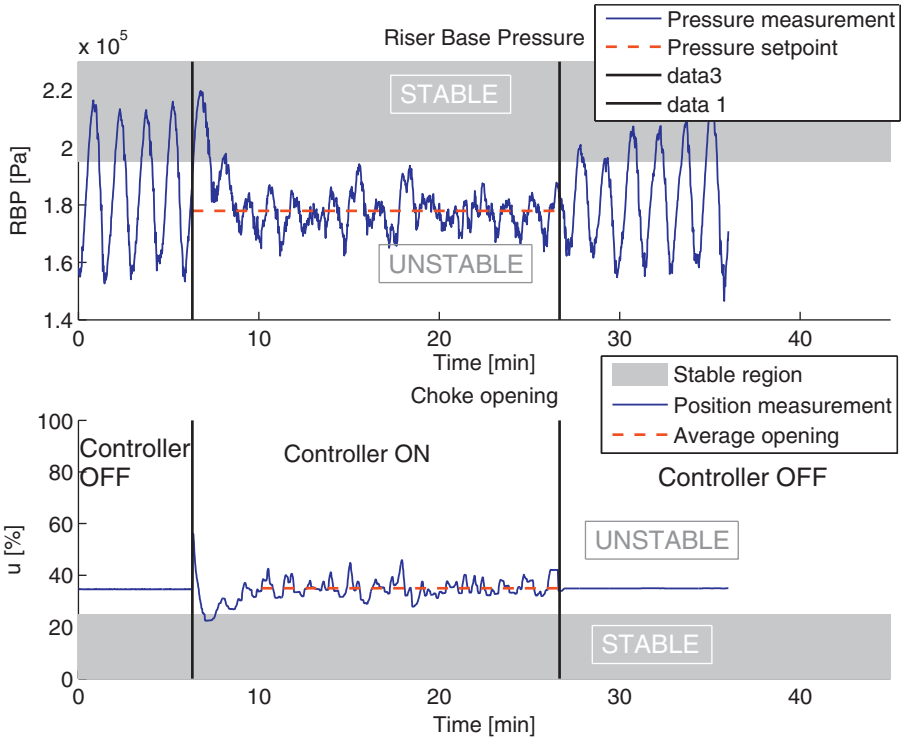

Fig. 15. Stabilization result for the nonlinear feedback law. The average valve opening after stabilization is 35%.

opening reached by Controller 4. As can be seen from this experiments, the use of the model-based control law compensates for the absence of a bottom pressure sensor. The average valve opening is slightly lower than with Controller 2, but because of slight modifications in the experimental setup, it corresponds to a slightly lower bottom pressure set point.

7. Conclusion

The results of these experiments, presented in Table 1, highlight the potential of the proposed control solutions, which overcome two important shortcomings of the reference PI controller: they are able to stabilize the flow for higher valve opening set points, and

provide a viable solution when no bottom sensor is available. In particular, the PI controller using as the output the pressure drop over the riser is an easily implementable control law, which does not require any additional sensor to the reference control solution (PI on the bottom pressure) or the use of the model. Besides, the proposed model-based nonlinear feedback law compensates almost fully the absence of a bottom pressure sensor.

The positive results of the model-based control solutions would probably be attenuated during real-scale implementations. In particular, the model may not be representative for a large range of operating points on a real well, where the inflows usually depend on the bottom pressure, whereas they are assumed constant in the model. Adaptive techniques or the incorporation of pressure-driven inflows to the model could overcome these difficulties. On-line adaptation could also be used to alleviate some of the off-line tuning effort, which remains rather tedious. Besides, the limitations imposed by unstable zeros when no bottom pressure sensor is available could reveal much more restrictive on a real system.

Finally, the list of possible controllers investigated in this article is by no means exhaustive. Future contributions should include the comparison with solutions involving other possible locations for the pressure sensors, in particular at the inlet of flowlines, as well as other types of sensors. In [31], it is shown that combinations of topside density, flow and pressure measurements can be used in cascade controllers to achieve stabilization. Interestingly, these types of measurements could enrich the model-based approach to yield even better results.

Appendix A. Parameters of the model

In this section, we detail the values of the parameters of the model resulting from the calibration process in each considered case. Besides, the following analytical expressions can be used to compute some of the parameters (for more details, the interested reader is referred to [27]) (Table A.2).

$$
\begin{aligned}
C_{out} &= \frac{w_{l,in}}{\overline{u}\sqrt{\overline{p}_{r,t} - p_s}} \\
m_{l,still} &= \frac{\overline{p}_{r,b} - \overline{p}_{r,t}}{g/A\sin\theta}\left(1 + \frac{\overline{p}_{r,t}}{bGLR}\right) - \frac{\overline{p}_{r,t}}{bGLR}V_r\rho_l \\
\epsilon &= \frac{\overline{p}_{r,t}}{bGLR}\frac{\rho_l V_r - (p_{r,b}^{max} - \overline{p}_{r,t})(A/g\sin\theta)}{(p_{r,b}^{max} - \overline{p}_{r,t})(A/g\sin\theta) - m_{l,still}}
\end{aligned}
$$

Table A.2
List of the model parameters used to match the well and loop slugging oscillations.

Parameter	Description	Value Oseberg field	Value test rig
R	Gas constant	8.314 J K	$8.314\,\mathrm{J\,K^{-1}\,mol^{-1}}$
T	Temperature	363 K	287 K
M	Molecular mass of gas	$2.2\times10^{-2}\,\mathrm{kg\,mol^{-1}}$	$2.9\times10^{-2}\,\mathrm{kg\,mol^{-1}}$
ρ_l	Liquid density	$900\,\mathrm{kg\,m^{-3}}$	$1050\,\mathrm{kg\,m^{-3}}$
g	Gravity constant	$9.81\,\mathrm{m\,s^{-2}}$	$9.81\,\mathrm{m\,s^{-2}}$
θ	Pipe inclination	$\pi/4$ rad	1.496 rad
D	Pipe diameter	1.5×10^{-1} m	7.6×10^{-2} m
A	Cross-section area	$4.4\times10^{-3}\,\mathrm{m^2}$	$1.8\times10^{-2}\,\mathrm{m^2}$
p_s	Separator pressure	6.6×10^5 Pa	1×10^5 Pa
$w_{l,in}$	Water inflow mass rate	$11.75\,\mathrm{kg\,s^{-1}}$	$2.0417\,\mathrm{kg\,s^{-1}}$
$w_{g,in}$	Air inflow mass rate	$8.2\times10^{-1}\,\mathrm{kg\,s^{-1}}$	$4.7\times10^{-3}\,\mathrm{kg\,s^{-1}}$
L	Length of the pipe	5200 m	15 m
ϵ	Fraction of inflow gas	0.78	0.01
C_{out}	Choke constant	$2.8\times10^{-3}\,\mathrm{m^2}$	$6.48\times10^{-5}\,\mathrm{m^2}$
$m_{l,still}$	Still mass of liquid	3.73×10^4 kg	32.9 kg
C_g	Virtual valve constant	1×10^{-4} m s	3.3×10^{-7} m s
V_{eb}	Volume of the elongated bubble	$48\,\mathrm{m^3}$	$0.558\,\mathrm{m^3}$

where $\overline{p}_{r,t}$ is the equilibrium value of the topside pressure corresponding to the valve opening $\overline{u}$, $\overline{p}_{r,b}$ is the corresponding value of the bottom pressure and $p_{r,b}^{max}$ is the maximum value of the bottom pressure oscillations. Finally, the value of parameter V_{eb} must be determined by solving the following nonlinear equation

$$\Re\{\lambda(u^*, V_{eb})\} = 0$$

where u^* is the bifurcation point of the studied system, and λ is one of the eigenvalues of the Jacobian of system (1)–(3).

Appendix B. Equilibrium of model (5)–(7)

First, one should notice that there can be no equilibrium for the whole system when the virtual valve is closed, that is to say when the expression inside the $\max(\cdot, 0)$ functions is negative. Thus, setting the left-hand-side of Eqs. (5)–(7) to zero yields the following expressions of the equilibrium

$$\overline{x}_1 = \frac{w_{g,in}}{C_g a} + \frac{\overline{x}_2}{a} + c\frac{\overline{x}_3 + m_{l,still}}{a} \tag{B.1}$$

$$\overline{x}_2 = p_s + \frac{1}{\rho_l}\left(\frac{w_{l,in}}{C_{out}\overline{u}}\right)^2 \tag{B.2}$$

$$\overline{x}_3 = \frac{\overline{x}_2}{\overline{x}_2 + b\epsilon(w_{g,in}/w_{l,in})}m_l^{\Delta} \tag{B.3}$$

As expected, the equilibria can be indexed by the values of $\overline{u} \in [0, 1]$.

Appendix C. Nomenclature

Table C.3 gives a brief description of the physical variables of the model.

Table C.3
Nomenclature.

Variable	Description
$m_{g,eb}$ (x_1)	Mass of gas in the elongated bubble
$m_{g,r}$	Mass of gas in the riser
$m_{l,r}$ (x_3)	Mass of liquid in the riser
$m_{g,r}/m_{l,r}$ (x_4)	Gas mass ratio in the riser
p_{eb}	Pressure in the elongated bubble
$p_{r,b}$	Pressure at the bottom of the riser (bottom pressure)
$p_{r,t}$ (x_2)	Pressure at the top of the riser (topside pressure)
w_g	Gas mass flow rate through the virtual valve
$w_{g,out}$	Gas mass flow rate through the outlet valve
$w_{l,out}$	Liquid mass flow rate through the outlet valve

References

[1] E. Blick, L. Boone, Stabilization of naturally flowing oil wells using feedback control, in: SPE Paper, 1986.
[2] F.P. Donohue, Classification of flowing wells with respect to velocity, Petroleum Transactions, AIME 86 (1930) 226–232.
[3] J.-M. Godhavn, M.P. Fard, P.H. Fuchs, New slug control strategies, tuning rules and experimental results, Journal of Process Control 15 (2005) 547–557.
[4] K. Havre, M. Dalsmo, Active feedback control as the solution to severe slugging, in: SPE Annual Technical Conference, 2001.
[5] Z. Schmidt, J. Brill, H. Beggs, Choking can eliminate severe pipeline slugging, Oil & Gas Journal 12 (1979) 230–238.
[6] M. Dalsmo, E. Halvorsen, O. Slupphaug, Active feedback control of unstable wells at the Brage field, in: SPE Annual Technical Conference, 2002.
[7] K. Havre, K. Stornes, H. Stray, Taming slug flow in pipelines, ABB review 4 (2000) 55–63.
[8] K. Bendiksen, D. Maines, R. Moe, S. Nuland, The dynamic two-fluid model OLGA: theory and application, SPE Production Engineering 6 (1991) 171–180.
[9] D. Ferre, V. Bouvier, C. Pauchon, TACITE physical model description manual, in: Rapport IFP, 1995.
[10] B. Jansen, M. Daslmo, L. Nøkleberg, K. Havre, V. Kristiansen, P. Lemetayer, Automatic control of unstable gas lifted wells, in: SPE Annual Technical Conference, 1999.

[11] L.S. Imsland, Output Feedback and Stabilization and Control of Positive Systems, Ph.D. thesis, Norwegian University of Science and Technology, Department of Engineering Cybernetics, 2002.
[12] E. Storkaas, Control Solutions to Avoid Slug Flow in Pipeline-riser Systems, Ph.D. thesis, Norwegian University of Science and Technology, 2005.
[13] F. Di Meglio, G.-O. Kaasa, N. Petit, A first principle model for multiphase slugging flow in vertical risers, in: Conference on Decision and Control, 2009.
[14] F. Scibilia, M. Hovd, R.R. Bitmead, Stabilization of gas-lift oil wells using topside measurements, in: Proceedings of the 17th IFAC World Congress, 2008, pp. 13907–13912.
[15] L. Sinègre, Dynamic study of unstable phenomena stepping in gas-lift activated systems, Ph.D. thesis, Ecole des Mines de Paris, 2006.
[16] G. Bornard, H. Hammouri, A high gain observer for a class of uniformly observable systems, in: Proceedings of the 30th IEEE Conference on Decision and Control, vol. 2, 1991, pp. 1494–1496.
[17] H.K. Khalil, Nonlinear Systems, 3rd ed., Prentice Hall, Upper Saddle River, NJ, 2002.
[18] J. Falcimaigne, S. Decarre, Multiphase Production, IFP Publications, 2008.
[19] C.P. Hale, Slug Formation, Growth and Decay in Gas–Liquid Flows, Ph.D. thesis, Imperial College of Science, Technology and Medicine, University of London, 2000.
[20] A. Bøe, Severe slugging characteristics; Part I: flow regime for severe slugging; Part II: Point model simulation study, Presented at Selected Topics in Two-Phase Flow, NTH, Trondheim, Norway (1981).
[21] Y. Taitel, Stability of severe slugging, International Journal of Multiphase Flow 12 (1986) 203–217.
[22] B. Hu, Characterizing gas-lift instablilities, Ph.D. thesis, Department of Petroleum Engineering and Applied Geophysics, NTNU, 2004.
[23] E. Zakarian, Analysis of two-phase flow instabilities in pipe-riser systems, in: Proceedings of Pressure Vessels and Piping Conference, 2000.
[24] P. Skousen, Valve Handbook, 3rd ed., McGraw-Hill, 2011.
[25] F. Di Meglio, G.-O. Kaasa, N. Petit, V. Alstad, Model-based control of slugging flow: an experimental case study, in: American Control Conference, 2010.
[26] E. Walter, L. Pronzato, Identification of Parametric Models from Experimental Data, Communications and Control Engineering Series, Berlin: Springer, 1997.
[27] F. Di Meglio, G.-O. Kaasa, N. Petit, V. Alstad, Reproducing slugging oscillations of a real oil well, in: 49th IEEE Conference on Decision and Control, 2010.
[28] M. Johansson, A. Rantzer, Computation of piecewise quadratic lyapunov functions for hybrid systems, IEEE Transactions on Automatic Control 43 (1998) 555–559.
[29] F. Clarke, Nonsmooth analysis in control theory: a survey, European Journal of Control 7 (2001) 145–159.
[30] P.E. Hedne, H. Linga, Suppression of terrain slugging with automatic and manual riser choking, in: Presented at the ASME Winter Annual Meeting, Dallas, TX, 1990.
[31] H. Sivertsen, E. Storkaas, S. Skogestad, Small-scale experiments on stabilizing riser slug flow, Chemical Engineering Research & Design 88 (2010) 213–228.